Active Sensing for High-Speed Offroad Driving*

Kayur Patel, Walter Macklem, Sebastian Thrun, Mike Montemerlo
Stanford AI Lab
Stanford University
Stanford, CA 94305
{*kdpatel,wmacklem,thrun,mmde*}*@cs.stanford.edu*

***Abstract*— In this paper we propose an active control strategy for scanning laser sensors on autonomous vehicles traveling offroad at high speeds. As speed increases the amount of sensor information about the terrain decreases. We address the problem of sensor control in the context of this speed-coverage trade off. The algorithm and testing methodologies are described with results comparing our active sensing method to a passive sensing method.**

***Index Terms*— active sensing, active perception, active vision, high speed, offroad**

I. Introduction

Perception is the key to high-speed offroad driving. A vehicle needs to have maximum data coverage on regions in its trajectory, but must also sense these regions in time to react to obstacles in its path. In offroad conditions, the vehicle is not guaranteed a traversable path through the environment, thus better sensor coverage provides improved safety when traveling.

Scanning lasers are the preferred sensor for offroad applications [8]. A disadvantage of a scanning laser is its limit in range and speed. Consequentially, lasers have limited spatial density of data [8]. At slow speeds under 5 m/s, a scanning laser sensor can collect enough data from the environment to fully sense the vehicle path. Therefore, the vehicle always has enough time to react to obstacles and is in a minimal amount of danger at any point. When the vehicle moves at high speeds greater than 10 m/s (22 mph), the vehicle can no longer sense its entire path and will travel over unknown regions. Traversing unknown regions on its trajectory is a calculated risk of traveling at high speeds.

A remedy for this problem is to increase the number of laser sensors. An alternative approach is to increase the utility of the existing sensors on the vehicle. One way to perform this is to actuate the sensors toward interesting features in the vehicle's environment, such as unknown regions on its current trajectory.

A passive sensing model is described as having either a sensor mounted that is:

- attached directly to the vehicle in a fixed position and orientation
- attached to the vehicle on a movable platform, such as a pan/tilt unit. This movable platform is actuated in a pre-defined motion, such as a sweeping arc motion.

Conversely, an active sensing model has a sensor mounted on a movable platform whose position and orientation is chosen to examine points of interest in the environment.

The active sensing model provides two distinct advantages over a passive sensing model. Regions of the environment that are not accessible to a passive sensor can be viewed by a moving active sensor. Unlike passive sensing, active sensing focuses the sensor's data on the most important regions.

Active sensing has been previously explored [6], [7], in particular with computer vision. The ability to orient a camera has increased the ability for 3-D shape parameterization, obtaining range from 2-D segmentation of an image [1], and recovering surface shape from occluding contours [3]. Active sensing with vision has also been used for improving data association within the SLAM problem [2]. Other recent papers have used sensing to smartly navigate through indoor and outdoor terrains [4], [9], [10].

Previous work has been done with sensor actuation for navigation and localization. Nabbe [4] has recently applied an active sensing strategy to the task of mobile robot planning and Burgard [14] has applied an active sensing strategy to the task of mobile robot localization. Both of these works have focused on identifying key points of interest in the terrain that, when coupled with active perception, will provide a better solution for navigation or localization. Neither addresses the issue of continuous active sensing for offroad navigation.

Much of the previous work in active sensing has been more static, in that there has been no time limit in which a region has to be sensed. However, autonomous driving is a temporal problem. The greater the distance at which the environment is perceived allows more time for the system to react and the safer the vehicle can travel on its trajectory. Active sensing allows an increased reaction time which is pivotal for high-speed offroad driving.

On-road autonomous driving has been feasible since the early 1990's [15]. Since then, there has been a considerable amount of interest in autonomous offroad driving [16]. However, little work has been done in high-speed offroad conditions [5], [17].

Sukthankar [13] performs active sensor control for a

* Thanks to Volkswagen for providing Stanford University with a vehicle and research support.

camera mounted on an autonomous vehicle which provides better coverage on sharp turns. However, this camera system has only been used on drivable roads and is unclear on its performance in an offroad setting at high speeds.

To the best of our knowledge, no prior work has successfully merged high-speed offroad driving with active sensing. The melding of these two issues is key for safe autonomous driving under these conditions.

At first glance, a greedy strategy that points the sensor at the nearest unknown region may seem optimal. However, this may inhibit the ability to sense upcoming cells. It is to the vehicles advantage to traverse one unknown region in order to see more later.

Our active sensing algorithm addresses the vehicle navigation problem by identifying key unknown regions in the trajectory that would be interesting to view. Our approach aims to minimize the number of unknown regions the vehicle traverses while traveling on a fixed way-point trajectory. The algorithm performs a lookahead search which picks the optimal direction to pan the laser according to a utility function. The utility function dynamically assigns value to each region based on distance from the vehicle and the ability of the laser to sense the region.

This paper will compare an active model for sensor actuation against a passive sensing model at high speeds in offroad conditions. If the vehicle is permitted to traverse a certain percentage of unknown regions on its trajectory, we will show that the active sensing model allows for better data coverage on its trajectory in comparison to a passive model. This increase in data coverage will allow the vehicle to travel at quicker velocities while maintaining a minimum level of unknown region traversal.

II. Method

At any given point in time, regions close to the vehicle are immediately important and require attention. Distant regions are less important because the laser has time to sense them in the future. However, as the vehicle begins to move, the temporal nature of the problem presents itself. Close regions matter less as they are traversed, and distant regions become close and more important. We incorporate this variable importance into a dynamic utility function.

Our dynamic utility function is an evaluation metric for a fixed horizon lookahead planner. The planner does a shallow lookahead search to estimate what the vehicle *will sense* in the near future. Based on the evaluation of the utility function, the vehicle chooses a direction to move its laser.

A. Traversability Map and Trajectory

A 2-D traversability map is an underlying structure for making decisions. 2-D traversability maps have been successfully used on offroad driving to interpret 3D data and create reasonable assessments of the terrain [5], [17]. Reducing dimensionality of the problem also allows for faster real-time algorithms.

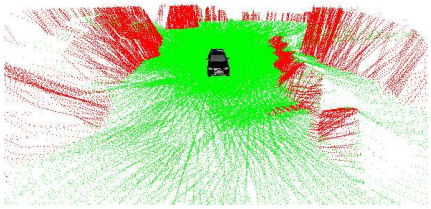

(a) A point cloud of our terrain.

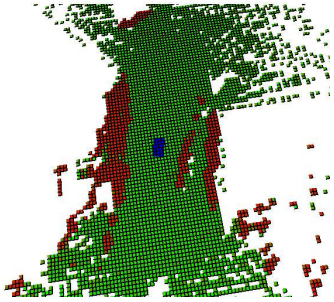

(b) A traversability map of the point cloud.

Fig. 1. The images above were gathered by moving the vehicle in the evaluation environment. The black object in the middle of (a) and the blue object in (b) is the vehicle. The green (light gray) areas and points are traversable regions. The red (dark gray) indicates obstacles.

The vehicle builds a map as it senses its environment. Each laser scan is converted into a set of points in the global coordinate frame. The points in a scan are compared to their neighbors and labeled. Points with sudden steep changes in z value are labeled as obstacles, otherwise they are labeled as free [15]. The points are placed into their corresponding grid cells and the status of the cell is updated in the standard manner. A picture of a point cloud and its corresponding map are shown in Figure 1.

The traversability map gives the status of the terrain, however all regions on the terrain are not of interest. We only care about regions of the terrain that will be hazardous to the vehicle as it performs it task. In our case, the task is to follow a fixed trajectory on the terrain.

The vehicle's trajectory is specified by a set of 2-D way-points. Each way-point is connected by a straight line to form a path for the vehicle to travel. We specify important regions as those along our trajectory. In terms of the traversability map, we create a corridor of cells which may be encountered by our vehicle as it travels between way-points.

Due to limitations in the speed of laser refresh and sensor actuation, at high speeds it becomes impossible to know the state of all of the cells in our trajectory corridor. Therefore, a successful trajectory run is one that minimizes the number of unknown cells traversed by the vehicle.

B. Active Sensing Method

As the vehicle runs its trajectory, the cells of interest and information about the terrain change. The goal is to be able to assimilate this information into a control strategy.

For the purposes of choosing a control direction, we simplify to a 2-D traversability map. The 2-D motion of the vehicle is estimated by moving it along the way-points. A single vertical scan is just a stripe of data in a straight line from the laser. In a 2-D setting, the data strip is just ray cast from the laser at the angle of the laser.

Given a 2-D vehicle and a laser angle, we estimate which cells are sensed by casting a fixed length ray over the traversability map. Figure 2 illustrates this process. Each ray returns a list of n grid cells in the order they are intersected by the ray. These grid cells $c_{1:n}$ make up a scan ray s.

The ordering of cells in s provides information about the distance of the cells from the vehicle. Closer cells are more important. However, pointing a sensor to the closest cell may inhibit the ability of the vehicle to sense distant cells. Since distant cells become close as the vehicle moves, knowing the future effect of moving the sensor is important.

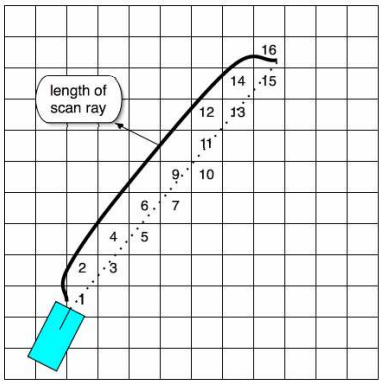

Fig. 2. The 2-D vehicle does a ray cast to compute a scan ray s. The length of the ray is set in the experiment and is constant for each ray. The scan ray comprises of the numbered cells in the order that they are numbered. For example this scan ray would contain cells $c_{1:16}$.

To estimate what the vehicle will sense, we must estimate how it moves across the terrain. Let $[\bar{r}, \bar{S}]$ **move**(r, D, i) be the function for moving the vehicle. The function takes as arguments a vehicle r, a direction to move our laser D, and a count i of how many scan rays to collect. For each scan ray gathered, the vehicle is moved, a ray is cast, and the intersecting cells are collected.

The 2-D pose has a translational velocity v and an instantaneous rotation, the laser has a rotational velocity ω_{pan}. Before moving, the v is updated by acceleration. The scan rate of the laser T (Hz) is known. The vehicle moves by $\frac{v}{T}$ and the laser pans in direction D by $\frac{\omega_{pan}}{T}$. When i scan rays have been gathered, **move** returns a vehicle at its current position $\bar{r}$ and a list of scan rays $\bar{S}$.

While scan rays can now be gathered for moving the laser in a given direction, there is only one decision point for choosing the direction of the laser. To improve its estimate, the planner takes into account multiple decision points.

TABLE I
SEARCH ALGORITHM

```
1:  float search(d, S, r, D)
2:      [r̄, S̄] = move(r, D, i)
3:      S' = S ∪ S̄
4:      if (d ≠ 0)
5:          return max_D̄(search(d − 1, S', r̄, D̄))
6:      else return U(S')
```

Our lookahead planner has two steps for its search. The first step involves the use of the **move** function. The search first moves the vehicle and collects a fixed number of scans rays. These scans rays are incorporated into a dynamically maintained list of scan rays S'. Based on the horizon of the search, the algorithm either branches or evaluates the utility of S'. The details of the algorithm are presented in Table I.

The search parameters given in line 1 include a list of scan rays S, a vehicle r, an actuation direction D, and a search depth d. The vehicle is moved in line 2 to gather a list of i scan rays $\bar{S}$ and a new vehicle $\bar{r}$. Lookahead time is based on the initial value of d, i, and the scan rate of the laser.

The current list of scans S is concatenated with $\bar{S}$ to create an updated list S'. If search has not reached a leaf node, it branches and returns the value of the maximum branch (lines 4-5). Otherwise it evaluates and returns the utility of S' (line 6).

The utility function evaluates the usefulness of a list of scan rays. Lists that are more likely to sense unknown cells on our trajectory are given higher values. The utility function is initialized by assigning the probability of sensing a cell to a small non-zero number.

Each scan ray $s \in S'$ consists of the list of map cells $c_{i:n}$ in the order that they are seen by a ray cast (Figure 2). The probability of sensing cell c_i given a scan ray is as follows:

$$\begin{aligned} p(c_i|s) &= p(c_i|c_{1:n}) && (1)\\ &= p(c_i|c_{1:i-1}) && (2)\\ &= p(c_i|c_{i-1})p(c_{i-1}|c_{1:i-2}) && (3) \end{aligned}$$

(1) expands s into its component cells. (2) assumes that sensing c_i is independent of sensing any cells after c_i. (3) assumes that given that c_{i-1} is sensed, sensing c_i is independent of any other cells before it. This leaves two terms. The first, $p(c_i|c_{i-1})$, is the probability of sensing c_i through c_{i-1}. The second, $p(c_{i-1}|c_{1:i-2})$ is the recursive step. Since there are no cells obstructing the view of c_1, $p(c_1) = 1$. Unrolling the recursion leaves:

$$p(c_i|s) = \prod_{j=2}^{i} p(c_j|c_{j-1})$$

$p(c_i|c_{i-1})$ is based on the classification of c_{i-1} in the occupancy map. The probability of sensing through an occupied cell is lower than sensing through a free cell. For simplification of the model, the case where the vehicle has the ability to sense over small obstacles has been ignored.

Since the cells in a scan ray are ordered from closest to farthest from the vehicle, cells further away will have a lower probability of being sensed. This is important for two reasons. First, cells that are close must be sensed before they are traversed. Secondly, since the laser gives more information about a close range, the vehicle is less likely to sense distant cells.

The probability of sensing a list of scans S' is the following:

$$\begin{aligned} p(c|S') &= p(c|s \cup S'') \\ &= 1 - \Big(1 - p(c|s)\Big) \times \Big(1 - p(c|S'')\Big) \end{aligned}$$

The list S is split into first scan ray s and the rest S''. Each scan ray is an independent observation of the cells, so the probabilities of multiple observations of the same cell are added. Since each scan ray is associated with a vehicle pose, cells that are far away in the current scan ray may be close in a future scan ray. Therefore we have a higher utility for not only cells that are close now but also cells that *will be* close in the future.

The utility is computed in the following manner:

$$U(S) = \sum_c p(c|S) 1\{c == unknown \wedge c \in trajectory\}$$

An indicator function, $1\{x\}$, is one if x is true and zero if x is false. We use the indicator to only consider areas that are unknown on the trajectory. The cells are further weighted by the probability of seeing them given our list of scans rays S.

The planner uses the search to choose a direction D by the following:

$$D = \arg\max_{D'} \textbf{search}(d, \{\}, r, D')$$

The search is initialized with an empty list of scan rays and the direction is chosen according the maximum value over all candidate directions D'.

C. Evaluation Environment

Comparing the relative effectiveness of different sensing modalities requires repeated runs over the same terrain. Changing environments, safety concerns, and time constraints make these comparisons impossible. To make our results more informative, we use vast amounts of prerecorded 3D data to create a systematic evaluation environment. In this environment we can develop algorithms and meaningfully compare them.

We gathered laser data from a Sick LMS mounted on a VW Touareg (Figure 3(a)). Pose data from various pose estimation devices was integrated through a Kalman filter. Using the laser data and the pose information we created a point cloud of the terrain (Figure 4(a)).

A height grid, with cell size of half a meter, is created with points placed into their respective cells. The z value for each cell is the average z for cells with low variance and the maximum z for cells with high variance. Each grid cell is represented by a point that consists of its center x, center y, and z values. Empty grid cells are interpolated using data from adjacent cells. Grid points are then connected with each other to create a terrain mesh. The terrain mesh still retains the obstacleness of the original terrain, but in a slightly coarser representation (Figure 4(b)).

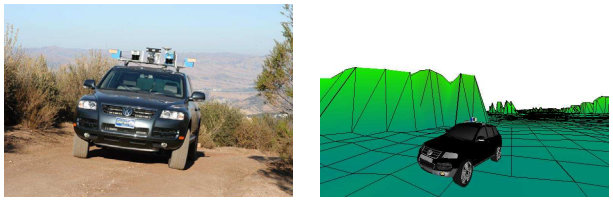

(a) vehicle (b) evaluation environment

Fig. 3. The VW Touareg

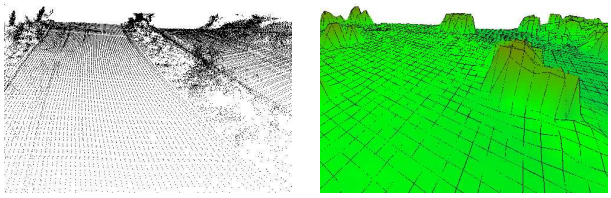

(a) Point Cloud (b) Terrain Mesh

Fig. 4. The protrusions in the point cloud and mesh correspond to trees. (a) Point Cloud of 3D data (b) Corresponding mesh overlay on top of point cloud.

The vehicle moves along our terrain by following a straight line way-point trajectory. The vehicle starts at rest and accelerates up to a maximum velocity. Our evaluation for the vehicle's pose is based on a 6-DOF vehicle estimation system.

The laser has an angular seperation of half a degree over a 180 degree spread. The laser is mounted such that it cuts a vertical plane in front of the vehicle. The laser pans left and right at a fixed velocity.

III. Results

A. Experimental Setup

To judge the effectiveness of our algorithm, we compare it to a passive sensing model. Passive sensing consists of panning the sensor left to right to sweep out an arc in front of the vehicle. The arc angle is also known as the field of view (FOV) of the laser.

Figure 5 displays the full vehicle trajectory. The trajectory consists of two 180 degree turns, two straight sections, and two sweeping gradual turns. In later testing, we felt the need to perform comparison tests specifically around a single curve. For these later runs, we truncated our trajectory to only include a single 180 degree turn.

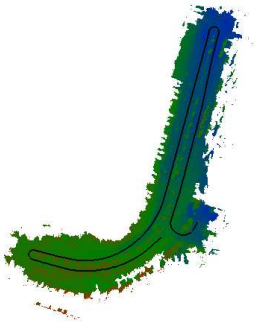

Fig. 5. The trajectory the vehicle traverses.

As the vehicle travels on its trajectory, it moves at a fixed maximum velocity. The vehicle starts at rest accelerating at a rate of 3 m/s^2 up to the fixed maximum velocity. The remainder of the trajectory is traversed at this maximum velocity. As the vehicle nears the final trajectory way-point, it decelerates to a resting position at a rate of 3 m/s^2. For braking, we assign μ = 1 for ground friction.

The laser is allowed to pan about the vehicle at a rate of π radians per second. The laser collects data from the environment at a rate of 25 Hz.

As will be discussed later, a vertically mounted laser provides sparse data coverage past 10 meters. Therefore, the length of the scanning ray was limited to 15 meters with no adverse effects on control. We chose to perform depth searches of $\frac{3}{5}$ of a second while allowing a direction branch every $\frac{1}{5}$ of a second (search depth, d, of 2). For the utility function, the parameter chosen for sensing a cell are as follows:

- If c_{i-1} is free, $p(c_i|c_{i-1}) = 0.9$
- If c_{i-1} is unknown, $p(c_i|c_{i-1}) = 0.9$
- If c_{i-1} is an obstacle, $p(c_i|c_{i-1}) = 0.1$

We performed a test run for every fixed maximum velocity between 3 to 20 m/s at 1 m/s increments. For passive sensing, we also varied the field of view of the laser between 10 and 90 degrees in 5 degree increments.

There are two different definitions for traversing an unknown cell. The first definition is if the vehicle physically passes over an unknown cell. The second definition involves the ability to react to a dangerous cell. While there are many ways to react, we chose braking distance to test our algorithm. The vehicle traverses an unknown cell if it cannot stop in time to avoid crossing the cell. The stopping distance s is based on the velocity v, acceleration a, and the friction μ of the ground.

$$s = \frac{v^2}{2\mu a}$$

B. Discussion

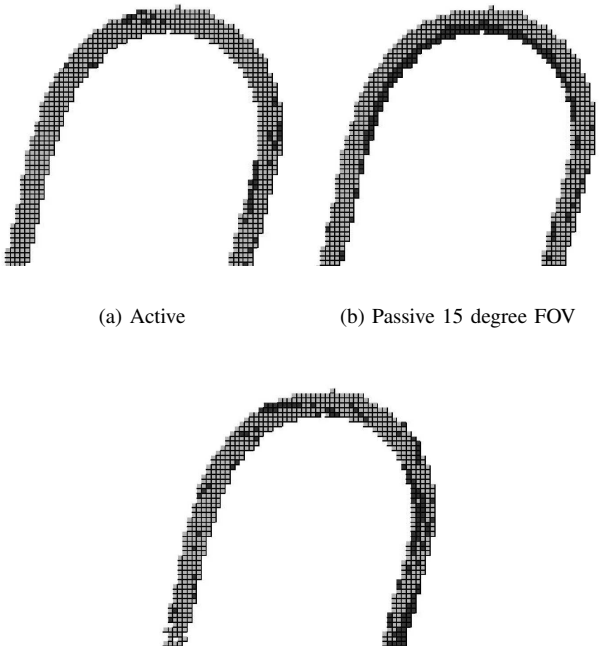

(a) Active (b) Passive 15 degree FOV

(c) Passive 75 degree FOV

Fig. 6. This grid shows a 180 degree curved trajectory that has been traversed by the vehicle. Dark cells in the grid indicate unknown cells and light cells in the grid indicate known cells. (a) Active sensing model (b) Passive sensing model with narrow FOV (c) Passive sensing model with wide FOV

Figure 6 contains visuals comparing our active control model with narrow and wide FOV passive models. A wide FOV gives more data about the cells on the edge of the corridor but covers many areas off the trajectory. Rays from a narrow FOV fall on cells of interest more frequently but may not see all of the cells on the corridor.

The grid in each figure represents a 180 degree curved trajectory through which the vehicle has already traversed. The light cells are areas in the trajectory that have been sensed and the dark cells are areas in the trajectory that are unknown. These tests were performed at a velocity of 15 m/s.

From Figure 6(b), we can see that the narrow FOV passive perception model misses large areas of the trajectory, particularly on the inside of the curve. As the vehicle drives around the curve, the narrow field of view only allows the sensor to perceive objects directly in front of the vehicle, thus it misses much of the inside track of the curve as it progresses.

Figure 6(c) illustrates a wide FOV passive perception model. This model performs better than the narrow FOV model around the curve, but the greater sweeping radius

results in a lower frequency of sensing directly in front of the vehicle. The wide FOV also wastes part of its cycle viewing areas on the outside of the curve that are of no importance to the vehicle.

Figure 6(a) illustrates the active sensing model. As it traverses the curve, it is able to maintain the sensor focus on the curved trajectory. This results in fewer missed cells in comparison to either of the passive sensing models.

Figure 7(a) illustrates test runs of the passive sensing strategy. Each line in Figure 7(a) represents the vehicle's velocity from 3 to 20 m/s. For each velocity, we changed the laser FOV in five degree increments and recorded the percentage of unknown cells that the vehicle traversed. The black circles for each velocity indicate the laser FOV that provided the minimum percentage of unknown traversed cells. For easier viewing, the black circles have been replotted in Figure 7(b).

At faster velocities, we see that the minimum FOV provides the best passive sensing strategy. The vehicle is moving quickly enough that is cannot sense the entire trajectory and a minimum FOV provides a greater density of data in front of the vehicle. As the velocity decreases, the vehicle is able to sense the entire path directly in front of it on a straight trajectory, thus the wide FOV provides greater advantage on the curved trajectory.

In Figure 8, we plotted the black indicator line for the optimum FOV from Figure 7(b) against our own active sensing control algorithm. Active sensing consistently outperforms the passive sensing model by a signficant margin and particularly excels between the two to six unknown percentage areas.

One would expect that a passive sensing algorithm with a narrow FOV would rival an active sensing strategy on straight regions of the trajectory. In fact, when viewing the algorithm in action on a straight section, we see that the active sensing strategy mimics passive sensing by performing a consistent sweeping motion across the planned path. Straight trajectories do not take advantage of the power that active sensing provides.

In Figure 9 we truncated our trajectory to only contain a single 180 degree turn. We again found the fixed perception optimum FOV for each velocity and plotted against active perception. As previously seen in Figure 6, the active sensing model significantly outperforms the passive sensing model.

Table II lists the metrics that are plotted in Figures 8 and 9. By maintaining a relatively low percentage unknown (between 4 and 6 percent), we can travel at fairly quick velocities using passive or active sensing. We see that active outperforms passive on the full trajectory, but provides a significant advantage on the curved trajectory. By maintaining a certain fixed percentage unknown around the curve, the active sensing model allows double the velocity as the passive sensing model.

Up to this point, the data has been the percentage of unknown areas the the vehicle has passed over. It is much

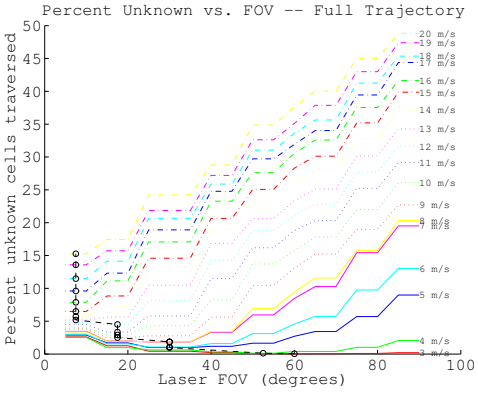

(a) Passive sensing's performance on the full trajectory

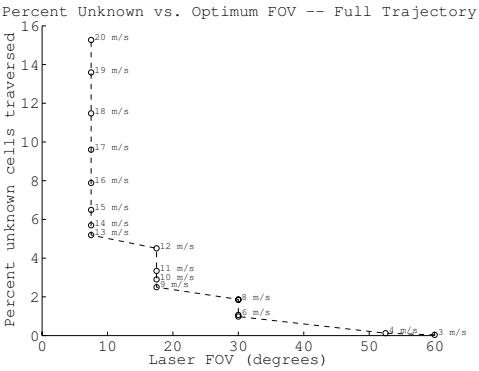

(b) Passive sensing's optimum FOV

Fig. 7. (a) Finding the optimum FOV for passive sensing at various velocities (b) Plotting the optimum FOV for each velocity

TABLE II

VELOCITIES ALLOWED PER FIXED PERCENTAGE UNKNOWN

Percent Unknown	*Full Trajectory*		*Curved Trajectory*	
	Passive	*Active*	*Passive*	*Active*
3	10.2 (m/s)	12.5	4.8	7.3
4	11.6	13.8	5.6	11.4
5	12.7	13.9	6.2	12.7
6	13.0	14.1	7.0	13.8

more interesting to explore the option of not only viewing the cells, but the necessity to the view the cells in enough time to react. In Figure 10, we explore the ability of braking distance. As shown, the percentage of unknown traversed areas quickly scales with velocity. At 3 m/s, we can view almost all areas before the required braking distance. But even as velocity approaches over 5 m/s, the percentage of unknown areas has already reached 50%.

This is a problem prone to using a vertically mounted sensor. As the laser scans a vertical stripe in front of the vehicle, the laser gather a considerable amount of data within the 5 meter range of the vehicle. But as the scan progresses outwards, the data density quickly drops. Past

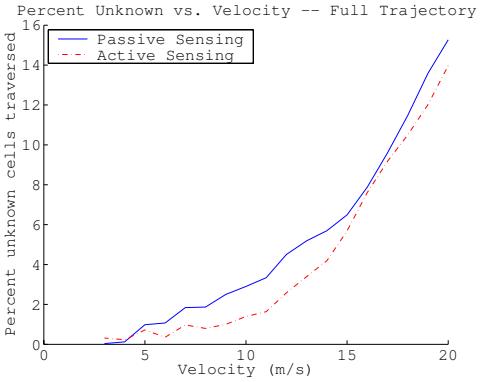

Fig. 8. Passive vs. active on the full trajectory

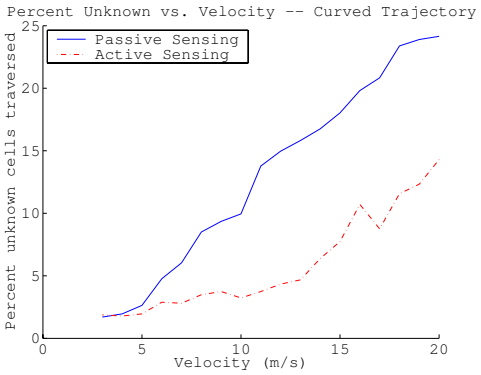

Fig. 9. Passive vs. active around the curved trajectory

the 10 meter range, the laser provides very sparse data converage.

When we increase the velocity of the vehicle past 3 m/s, the braking distance will far exceed the sensor's view. In most cases, using active perception will gain us an average of 0.5 m/s increase in velocity for the same percentage of unknown traversed regions.

This data must be taken with a grain of salt. We have a very conserative estimate of the deceleration of the vehicle. Furthermore, other metrics for reaction, such as swerving distance, can be considered and require less lookahead. The data is presented to show the active model still outperforms the passive when considering reaction time.

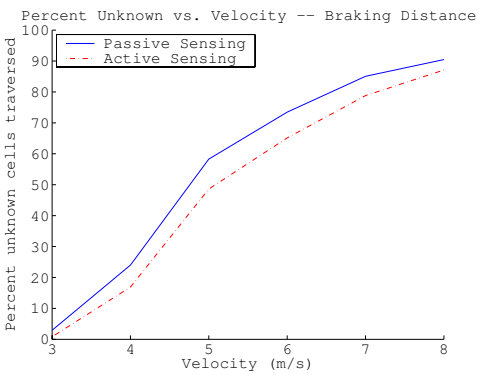

Fig. 10. Passive vs. active with braking distance

IV. Summary

In this paper we presented a method for actively controlling the laser sensor for high speed navigation. Our algorithm aims to minimize the number of unknown cells the vehicle traverses while traveling on a fixed way-point trajectory. The algorithm performs a look ahead search which branches on the direction to pan the laser. Each direction is assigned a utility based on a heuristic dependent on the probability of viewing unknown cells on our trajectory.

The algorithm was tested against the passive model of fixed panning along a field of view. Our results showed that for an acceptable percentage of unknown cells, active perception allows us to drive faster than the passive model.

References

[1] R. Bajcsy, "Active Perception", Proceeding of the IEEE, vol. 76, no. 8, August 1988.

[2] A. Davison, D. Murray, "Simultaneous Localisation and Map-Building Using Active Vision", IEEE Transactions on Pattern Analysis and Machine Intelligence, July 2002.

[3] K. Kutulakos, C. Dyer, "Recovering Shape by Purposive Viewpoint Adjustment", International Journal of Computer Vision, vol. 12, issue 2/3, March 1994.

[4] B. Nabbe, M. Hebert, "Where and When to Look", IROS 2003, October 2003.

[5] D. Coombs, K. Murphy, A. Lacaze, S. Legowik, "Driving Autonomously Offroad up to 35 km/h", Proceedings of the 2000 Intelligent Vehicles Conference, October 2000.

[6] J. Aloimonos, I. Weiss, A. Bandopadhay, "Active Vision", Internation Journal on Computer Vision, pp. 333-356, 1987.

[7] D. Ballard, "Animate Vision", Artificial Intelligence, vol. 48, no. 1, pp. 1-27, February 1991.

[8] M. Hebert, "Active and Passive Range Sensing for Vehicles", Proceedings of the 2000 IEEE Internationl Conference on Vehicleics and Automation, vol. 1, pp. 102 - 110, April 2000.

[9] H. Gonzalez-Banos, J. Latombe, "Vehicle navigation for automatic model construction using safe regions", Proceedings of Internation Symposium on Experimental Vehicles, pages 405-415, 2000.

[10] H. Gonzalez-Banos, J. Latombe, "Navigation strategies for exploring indoor environments", International Journal of Vehicles Research, 2002.

[11] A. Davison, "Mobile Vehicle Navigation Using Active Vision", Thesis for Ph.D. at the University of Oxford, 1999.

[12] J. Wann, D. Swapp, "Where do we look when we steer and does it matter", Journal of Vision, December 2001.

[13] R. Sukthankar, D. Pomerleau, C. Thorpe, "Panacea: An Active Sensor Controller for the ALVINN Autonomous Driving System", Proceedings of International Symposium on Vehicles Research, 1993.

[14] W. Burgard, D. Fox, S. Thrun, "Active Mobile Vehicle Localization", Technical Report IAI-TR-97-3, University of Bonn, Institut fr Informatik III, 1997.

[15] D. Pomerleau, "Efficient Training of Artificial Neural Networks for Autonomous Navigation", Neural Computation 3:1, pp. 88-97, 1991.

[16] I. Schwartz, "PRIMUS: an autonomous driving vehicle", Proceedings of the SPIE Vol. 3693 AeroSense Session on Unmanned Ground Vehicle Technology, 1999.

[17] C. Urmson, J. Anhalt, M. Clark, T. Galatali, J.P. Gonzalez, J. Gowdy, A. Gutierrez, S. Harbaugh, M. Johnson-Roberson, H. Kato, P.L. Koon, K. Peterson, B.K. Smith, S. Spiker, E. Tryzelaar, and W.L. Whittaker, "High Speed Navigation of Unrehearsed Terrain: Red Team Technology for Grand Challenge 2004", tech. report TR-04-37, Vehicles Institute, Carnegie Mellon University, June, 2004.